

Response to referee comments on “The added value of new ground-based observations in improving China’s methane emission quantification”

We thank the two referees for their careful reading of the manuscript and the valuable comments. This document is organized as follows: the referees’ comments are enclosed by rectangles, our responses are in plain text, and all the revisions in the manuscript and supplementary information are shown in blue. The line numbers in this document refer to the updated manuscript.

Reviewer #1

General comments

The manuscript evaluates the improvement in methane inversions over China resulting from the addition of new ground-based observations. The study is thorough, novel, and well-written, addressing an important issue in methane observations and emission inversions. I recommend it for publication in AMT, subject to a few minor revisions and clarifications.

From equations 3-4, the DOFs largely depend on the relative values of the observational error and the prior error. The formulation of the observational error will therefore influence the results. I suggest providing a detailed explanation of how the observational error is calculated: First, equation 2 for the observational error may be incorrect. According to Heald et al. (2004), Equation 2 calculates the observation error (ϵ_o), not the standard deviation of the observation error (σ_o). This appears to be a typo, but the authors should review the code to ensure the calculation is correct.

In addition, Heald et al. (2004) describe subsequent procedures: after calculating the standard deviation of the observation error, the relative residual standard deviation (RSSD) is computed by dividing the mean of the observations. The error variance for each observation is then calculated as $(y \cdot \text{RSSD})^2$. If the authors calculate the observational error based on the same procedures, I suggest the authors include these detailed steps in the manuscript.

Second, in Section 3.1 (line 310), the authors assume $\sigma_o = 65 \text{ppb}$ for each new station. Based on the procedure above, it may be preferable to assume a constant RSSD for the new stations rather than a fixed σ_o . This RSSD could be estimated using the six urban sites or other methods. Then, the observational error can be calculated as the model-simulated value multiplied by the RSSD, since the model generally captures spatial and seasonal variations of CH₄. I suggest the authors test this approach, or other reasonable assumptions, for weekly or monthly observations to illustrate the potential uncertainties arising from observational error assumptions.

Response. Thanks for these insightful comments. To address them, we have made the following changes.

1. Correction of Equation (2):

Thanks for pointing out the typo in Equation (2). We have corrected it in this manuscript.

Line 196. For S_o , we calculate the observational error standard deviations (σ_o) using the residual error method (Heald et al., 2004). The residual error (ϵ_o) is defined as the difference between observations (y) and GEOS-Chem

prior simulations (y_a), after removing the mean model bias ($\overline{y - y_a}$), as expressed in Eq. (2). The standard deviation of ε_O then gives σ_O (see Table 1).

$$\varepsilon_O = y - y_a - \overline{y - y_a} \quad (2)$$

2. Implementation of the relative residual standard deviation (RRSD) method:

To address the reviewer's concern and align more strictly with the relative residual error (RRE) method described in Heald et al., (2004), we have re-calculated the observational error variance for six urban sites using the relative residual standard deviation (RRSD) method. The RRSD is defined as the standard deviation of the residual error divided by the mean modeled methane concentration. We have incorporated the following description along with Fig. S2 and Fig. S6 to the revised manuscript:

Line 210. In part of the analysis, to account for the potential dependence of observational error on methane concentrations, we calculate the relative residual standard deviation (RRSD) as the standard deviation of the residual error (σ_O) divided by the modelled annual mean methane concentration in each grid cell. We adopt a reference RRSD of 3.3%, derived from six existing urban sites (Fig. S2). Thus, the hourly observational error ($\varepsilon_{O,i}$) is calculated as:

$$\varepsilon_{O,i} = RRSD \times y_{a,i} \quad (3)$$

where $y_{a,i}$ is the modeled methane concentration at hour i .

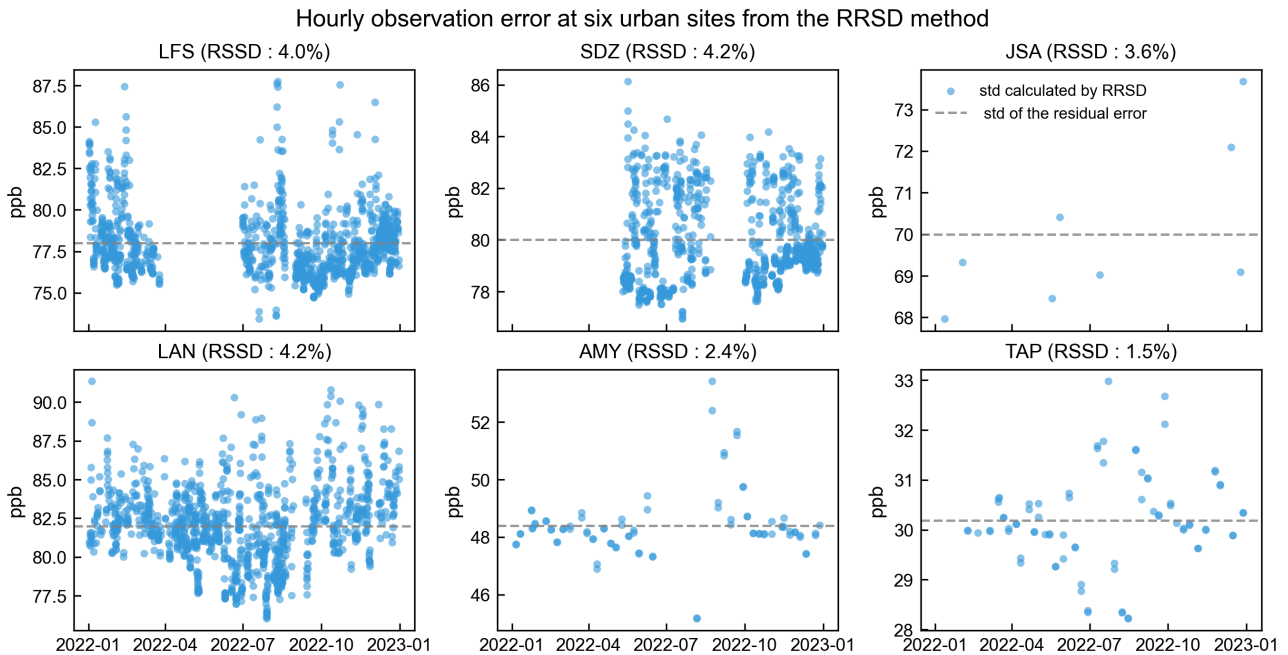


Figure S2. Hourly error at six existing urban stations derived from the relative residual standard deviation (RRSD) method. Gray dashed lines represent the standard deviation of the residual error. Blue dots denote the observation-specific error standard deviations calculated using the RRSD method (see Section 2.4 for details).

Line 479. We also solve for the optimal locations using the error standard deviations calculated from the RRSD method under a weekly sampling assumption (Fig. S6). The resulting spatial distribution of the newly added stations

is largely consistent with that obtained using a fixed standard deviation of 65 ppb.

Optimized surface station networks for weekly sampling frequency based on RRSd error characterization

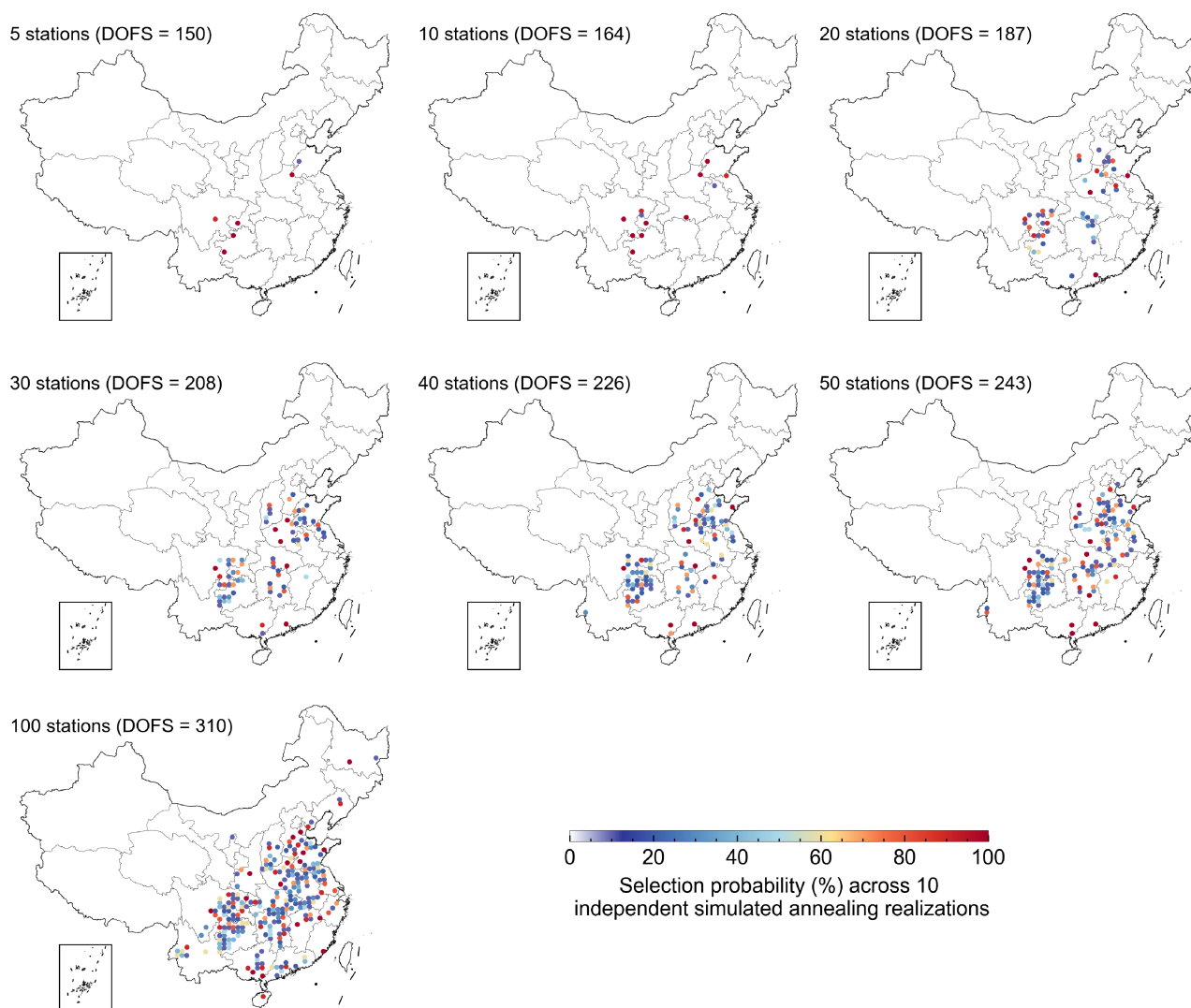


Figure S6. Optimized network expansion under weekly sampling when observation error is calculated by the relative residual standard deviation (RRSD) method. Panels show the selection probability (%) of each grid cell for a new site across 10 independent simulated annealing realizations, for network expansions of 5 to 100 new sites. The corresponding increase in the degrees of freedom for signal (DOFS) is displayed within each panel.

Other minor comments:

Line 155 (Section 2.4): Please clarify that the k-means clustering algorithm is applied to low-emission grid cells in China as well as all grid cells outside China.

Response. Many thanks for your constructive suggestions. We have clarified this in the text and included Table S1 to detail the factors used in the K-means clustering method.

Line 165. Our analysis preserves the native spatial resolution of high-emission grid cells ($>1 \text{ Gg a}^{-1}$), while low-emission grid cells ($< 1 \text{ Gg a}^{-1}$) are aggregated via K-means clustering to reduce computational cost. This clustering

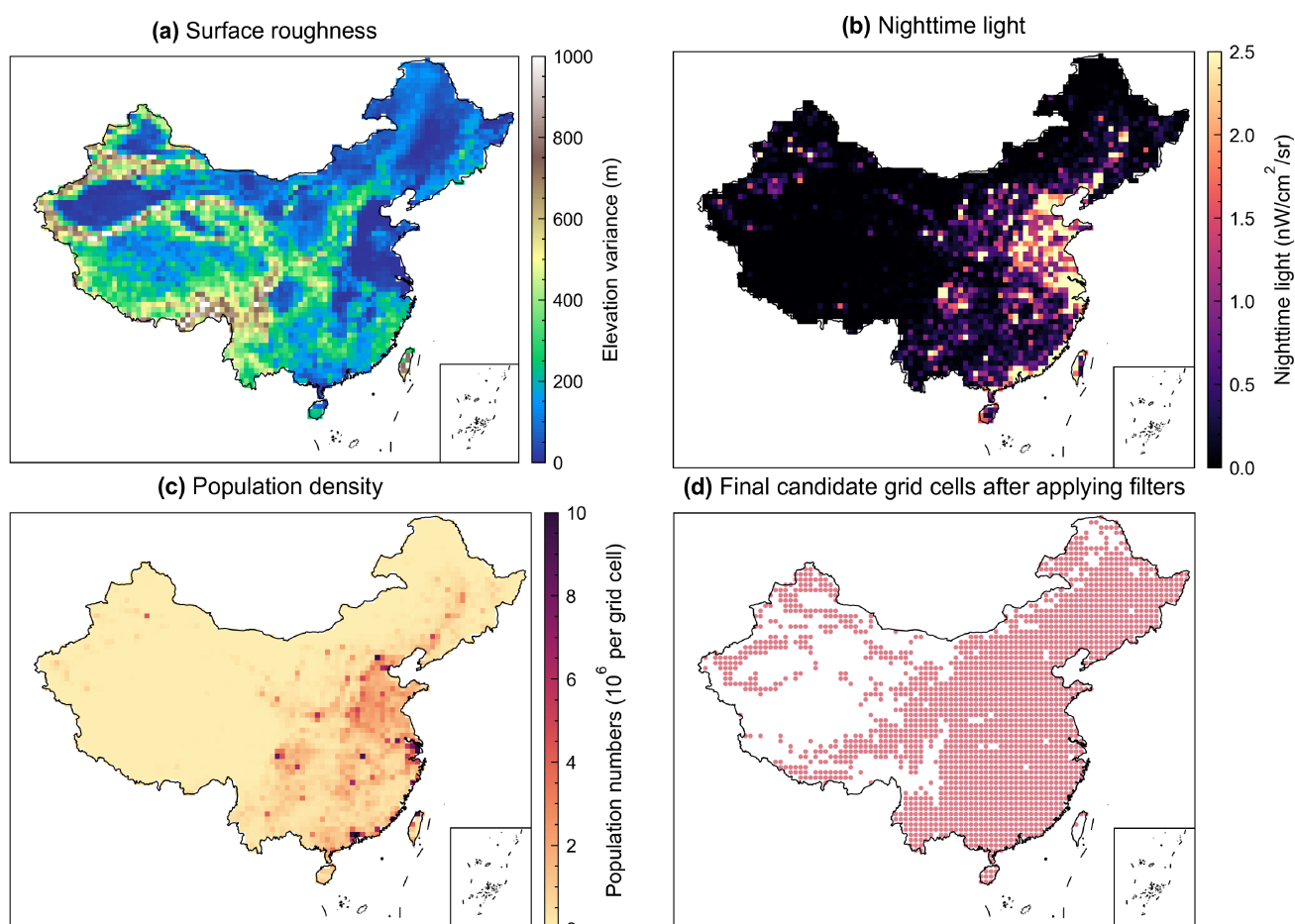
makes use of each gridcell's latitudes, longitudes and 10 sectorial emissions (see Table S1).

Table S1. Variables used in the K-means clustering algorithm for aggregating the low emission gridcells (< 1 Gg a⁻¹).

Category	Input variables	Processing	Description
Spatial coordinates	Latitude, longitude	Normalized to the range of 0–1.	To aggregate geographically proximate grid cells.
Sectorial emissions	10 Sector-specific emissions (e.g. Coal, oil, gas, livestock, rice etc.)	Normalized and weighted by sector contribution.	To group cells with similar emission-source profiles.

Fig. 3: Consider adjusting the color scale in Fig. 3b and clarifying the units in Figure 3c (e.g., 10⁶ per grid cell?).

Response. Thanks for your helpful suggestion. We have updated Fig. 3.



Line 468: The improvements for coal mining and biomass burning are minimal. Is this because the a priori sensitivity for coal mining is already large, and biomass burning emissions are too small? Some explanation of sector sensitivity

should be added.

Response. Thanks for your helpful suggestion. We have added the following description:

Line 580. The AK sensitivity of the inversion depends on emission magnitudes and observation density. For coal mining, the minimal improvement in AK when adding new sites is primarily because these large sources are already well-constrained by the current network, with AK values already nearing unity (Fig. 10). For biomass burning, the limited improvement is primarily due to its small emission magnitude ($\sim 0.2 \text{ Tg a}^{-1}$).

Fig.1: It would be helpful to show the regional divisions directly on this figure instead of in the supplementary (e.g., by adding bold lines).

Response. Thank you for pointing this out. We have updated Figure 1 by adding bold boundary lines to delineate the four study regions and removed the figure in the supplementary. The revised Figure 1 is attached below.

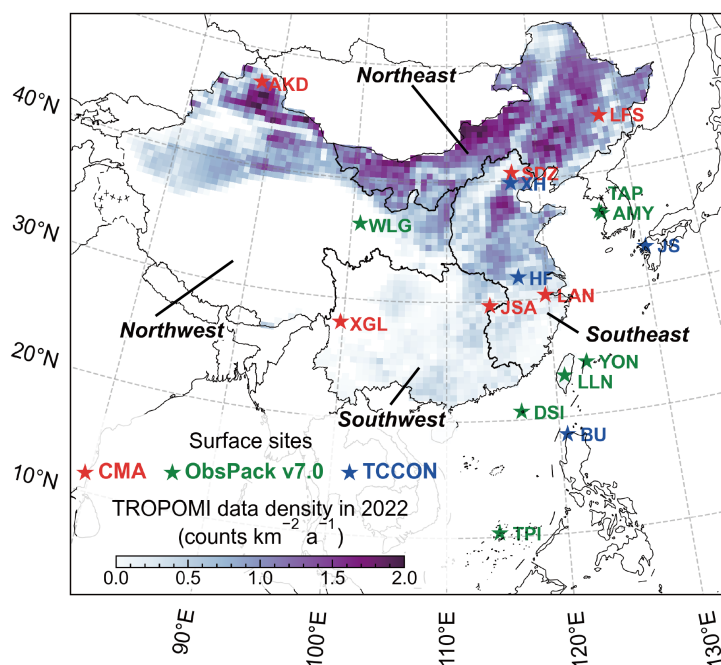


Figure 1. Spatial distribution of TROPOMI methane observation density ($\text{counts km}^{-2} \text{ a}^{-1}$) and ground-based monitoring stations for the year 2022. The surface stations are sourced from networks and databases including the China Meteorological Administration (CMA) (Fang et al., 2013; Wang et al., 2020; Zhang et al., 2022), NOAA GLOBALVIEWplus CH₄ ObsPack v7.0 (Schuldt et al., 2024) and the Total Carbon Column Observing Network (TCCON, 2022). The TROPOMI observation density is shown at $0.5^\circ \times 0.625^\circ$ horizontal resolution. Additional details regarding the surface site characteristics and TROPOMI observation information are provided in Table 1. The four regions (Northeast, Northwest, Southeast and Southwest) are spatially defined in Fig. 1.

Fig. 9: The background color seems to indicate uncertainty reduction. It is unclear what the color of the circles represents. Please clarify.

Response. Thanks for this suggestion. We have added the following description:

Line 531. The locations of the newly added stations are indicated by the black circles in the figure.